Interactions of a plasma and an incoming flow at Mach 3

Bruno Fornet, Guillaume Dufour, François Rogier

Interactions of a plasma and an incoming flow at Mach 3

B. Fornet[a] *, G. Dufour [a]and F. Rogier [a]

[a] ONERA, Centre de Toulouse
2, av. Edouard Belin BP 4025
31055 Toulouse Cedex 4 - France

A mechanical spike is a device used to mechanically act on the bow shock ahead of an airplane in supersonic flight. This action results in improved flight conditions. We will investigate here the effects of the axial generation of a two-hundred-micrometer width cylindrical plasma ahead a quasi-realistic nose profile of centimeter width. The device is named plasma spike by analogy to the above-cited mechanical device. This plasma spike is a source of both momentum and energy for the neighboring fluid.

1. Introduction

A central question in aeronautics is to improve the flight conditions of an aircraft. Among the different ways to go, various mechanisms of flow control have been investigated, both experimentally and numerically, during the last decades [9]. We are interested here in simulating the effects of a plasma actuator on a supersonic flow. In the studied device, a "virtual spike" appears as energy is deposited into the flow by a dense plasma coming from an electrodeless laser-guided discharge. This work is a first step towards a better understanding of the mechanisms at hand as well as the assertion of the expectable drag reduction.

Works on similar topics have been conducted for instance in [4], [6] and [7]. The authors of [4] propose a very detailed model in order to account for the effects of a Nd:YAG laser energy deposition in air for supersonic flow control. The process was modelled from the plasma generation by the laser to its interaction with the fluid ahead of a sphere. In [6], the authors study the effects of instantaneous energy deposition taken into account as fluid heating on a supersonic flow ahead of a cone. Parametric studies were led depending on the upstream flow velocity as well as the cone angle using a multi-domain WENO scheme to simulate 2-D axisymmetric Euler equations. The authors of [7] investigate the possibility of creating steering moments by off-axis plasma heat addition ahead of a cone. They use a 3-D fluid solver in order to do so for different kinds of heating processes and look at the effects of different parameters on the observed results.

Due to the specificities of the envisioned device, based on involved time scales, we assume as a first approximation that plasma generation is decoupled from its effects on the fluid. Under this assumption, one natural question is then to look at the effects of

*Acknowledgements: research funded by RTRA STAE/PLASMAX.

the introduction of a plasma of determined energy on the fluid. Answering this question would give us a good idea of what is needed to be done during plasma generation.

Another aspect would be to get a better understanding of the underlying mechanisms. The previous question is of central interest considering that the device we investigate should be used in a pulsed way. The specificities of our discharge allow us to propose a simplified, numerically cost-friendly model, aimed at answering the above questions. In order to do so, important coupling mechanisms between fluid and plasma have been investigated. This model is also intended for being the basis of a larger one integrating to some degree more accurate physics concerning the plasma-fluid interactions as well as the mechanisms behind plasma generation.

After explaining our modelling assumptions, we will comment the qualitative results they yield. In the asymptotics of small Debye length, we consider a two-fluid model with two temperatures [1]. This 2D-axisymmetric model couples the physics governing the plasma with compressible Euler type equations accounting for the fluid dynamics. Several time and space scales are involved in this problem as the plasma is by several orders of magnitude thinner and more reactive than the fluid as far as the densities are concerned.

2. The modelling assumptions.

We will detail here the assumptions made in order to obtain a simplified model, the one our simulations are actually based upon. Air chemistry is an intricate topic and in our case air will be seen as a fictive matter : to this end, we introduce a fictive air molecule (denoted A in what follows). The considered species are then the neutrals A, the first ionized state A^+ and the electrons e^-. The underlying kinetics are the ionization reaction:

$$A + e^- \mapsto A^+ + 2e^-,$$

and the three-body recombinations:

$$A^+ + e^- + e^- \mapsto A + e^-,$$

$$A^+ + e^- + A \mapsto A + A.$$

The reaction frequencies associated to these reactions, given in s^{-1}, are respectively denoted ν_i, $\nu_{rc,n}$ and $\nu_{rc,e}$. Their expressions are detailed in the appendix.

Consequently the conservation of mass for the different species can be expressed as:

$$(1)\ \partial_t n_e + \nabla.(n_e v_e) = n_e(\nu_i - \nu_{rc,n} - \nu_{rc,e}),$$

$$(2)\ \partial_t n_+ + \nabla.(n_+ v_+) = n_+(\nu_i - \nu_{rc,n} - \nu_{rc,e}),$$

$$(3)\ \partial_t n_n + \nabla.(n_n v) = -n_n(\nu_i - \nu_{rc,n} - \nu_{rc,e}).$$

We are interested in a dense plasma, which implies it has a small Debye length. We opt then for a quasi-neutral model, which is valid in the limit of small enough Debye length. Practically we assume that, at the scale of every considered volume, the local density of positive charge equilibrates the density of negative ones: $n_e = n_+$.

Due to elastic collisions with the neutrals, we have $v_+ \simeq v_n$. We choose to take $v_+ = v_n$.

Moreover the flux of charged particles $\Gamma := -e(n_e v_e - n_+ v_+)$ is assumed to be divergence free in order to ensure the conservation of the charge.

As commonly assumed as a first approximation (congruence assumption [8]), the electronic flux Γ is close to zero which leads in turn to the velocity v_e being close to the velocity of the neutrals v_n, modulo a diffusive correction (ambipolar diffusion assumption):

$$v_e = v_n - D_a \frac{\nabla n_e}{n_e}.$$

Concerning the temperature of ionic molecules, we assume that $T_+ = T_n$. Hence no equation relative the state of the ions needs to be computed. More precisely, the quantities whose evolution needs to be computed are: (n, v, T) for the fluid, where $n := n_n + n_+$ is the density of heavy particles, $v := v_n = v_+$ is the velocity of heavy particles and $T := T_n = T_+$ their temperature. For the electromagnetic field, we are in a case where magnetic effects are negligible. The electric field will not be solved here but considered as a parameter acting as a source of energy for the electrons. We get then the following system of equations, where $p := nk_BT$ denotes the fluid pressure and $p_e := n_e k_B T_e$ the electronic pressure.

$$\begin{cases} \partial_t n + \nabla.(nv) = 0, \\ \partial_t (nv) + \nabla.(nv \otimes v) = \mathcal{S}^{mov}, \\ \partial_t \left(5/2p\right) + \nabla.\left(7/2pv\right) = \mathcal{S}^{NRJ}. \end{cases}$$

$$\begin{cases} \partial_t n_e + \nabla.(n_e v) - \nabla.(D_a n_e) = \mathcal{S}_e^{chem}, \\ \partial_t \left(3/2p_e\right) + \nabla.\left(5/2p_e u_e\right) - \nabla.(\lambda_e \nabla T_e) = \mathcal{S}_e^{NRJ}. \end{cases}$$

The source term accounting for the momentum transfer from the plasma to the fluid is:

$$\mathcal{S}^{mov} = n_e \nu_e (v_e - v),$$

the energy transferred from the plasma to the fluid is described by:

$$\mathcal{S}^{NRJ} = 2\frac{m_e}{m_{air}} k_B n_e \nu_e (T_e - T) + n_e e \nu_{rc,n} W_i,$$

the plasma kinetics are taken into account through:

$$\mathcal{S}_e^{chem} = n_e(\nu_i - \nu_{rc,n} - \nu_{rc,e}),$$

and the plasma energy balance is expressed by:

$$\mathcal{S}^{NRJ} = -2\frac{m_e}{m_{air}} k_B n_e \nu_e (T_e - T) + n_e e (\nu_{rc,n} - \nu_i) W_i.$$

3. Numerical aspects.

2-D axisymmetric simulations were performed using a compressible fluid solver coupled with a plasma solver. For time iteration in our fluid solver, we use the block inversion spatially split approximate factorization scheme. As a limiter, Venkatakrishan's is used. The chosen structured fluid solver allows to solve Navier-Stokes as well as Euler equations. As presented above we will consider here a non-viscous model for the fluid. The grid we use is refined on the Mach cone as well as on the axial area containing the plasma. Globally, the method chosen is based on Finite Volumes and the integration in time is implicit for the fluid and explicit for the plasma. For the plasma, the MUSCL scheme is used for the computation of the convection terms. The source terms describing the interactions between fluid and plasma are treated explicitly. Finally, due to the strong multiscale feature of the problem at hand, the behaviors of the plasma and the fluid are solved on different time and space scales.

We use subcycling for the time integration and a finer, precisely localized grid to solve the plasma behavior. These results are then averaged on a rougher grid used for the computation of the fluid behavior.

Let us detail our interpolation procedure. In a conical area around the axisymmetric axis $r = 0$, the 2-D plasma mesh and the 2-D fluid mesh are the same in the axial direction, while, in the radial direction the plasma mesh is much thinner and covers only a small part of the fluid mesh ($r \leq 600\mu m$). We use then linear interpolation in the radial direction. By testing different meshes, we checked that enough points were taken for the fluid grid in the plasma channel in order to get accurate results. We underline that the same mesh is used to search for a stable state and to test the plasma effects. Due to the local refinement needed near the plasma column, studying properly convergence towards a stable state is already an issue.

As both the time step and mesh are different for fluid and plasma we use the prime superscript for the plasma. For instance $n^k_{e,(i',j')}$ denotes the electronic density on the cell whose center is $(r_{i'}, z_{j'})$ at time t^k. t^k is the physical time reached after k time iterations on the fluid.

Schematic presentation of the different steps of our algorithm.

- **Plasma initialization**
  - Read fluid mesh.
  - Generation of plasma mesh.
  - Initialization of plasma variables: $n^0_{e,(i',j')},\ v^0_{e,(i',j')},\ T^0_{e,(i',j')}$.
- **Fluid initialization**
  - Read fluid mesh.
  - Initialization of fluid variables: $n^0_{(i,j)},\ v^0_{(i,j)},\ T^0_{(i,j)}$.
  - Read boundary conditions.
  - Read initial time step.
  - Read total iteration number.

- **Plasma time iteration** $t^{k'} \mapsto t^{k'+1}$ **on grid** $(r_{i'}, z_{j'})$

  - Interpolation of $n^k_{(i,j)},\ v^k_{(i,j)},\ T^k_{(i,j)}$ on $n^k_{(i',j')},\ v^k_{(i',j')},\ T^k_{(i',j')}$.
  - Evaluation of $v^{k'}_{e,(i',j')}$.
  - Computation of $\delta t' = t^{k'+1} - t^{k'}$.
  - Computation of $v^{k'+1}_{e,(i',j')}$ and $T^{k'+1}_{e,(i',j')}$.

- **Fluid time iteration** $t^k \mapsto t^{k+1}$ **on grid** (r_i, z_j)

  - Resolution of fluid equations without source term.
  - Test of plasma activity: if plasma still active do steps 3/ through 6/.
  - Plasma time iteration gives $n^k_{e,(i',j')},\ v^k_{e,(i',j')},\ T^k_{e,(i',j')}$.
  - By interpolation we get $n^k_{e,(i,j)},\ v^k_{e,(i,j)},\ T^k_{e,(i,j)}$.
  - Explicit time iteration: $Sources * \delta t$ added to solution obtained at step 1/.
  - If $|Sources * \delta t|$ is small enough, choose $\delta t^{k+1} > \delta t^k$.

4. The simulated experiment.

In this work we are interested in the effects of energy and momentum deposition on a flow. We choose to focus on commenting qualitatively the observed effects. The considered dimensions of our profile are analogous to ones we could choose for a physical experiment. We first perform an aerodynamic simulation that converges towards a stable state.

As we assume that a dense plasma appears instantaneously, the mechanisms of creation and sustainment of the plasma are not investigated. We assume that the created plasma has properties similar to the one observed in thunder. Namely, we take:

$n_e = 10^{24} m^{-3}, T_e = 30000K.$

As described above, the electronic velocity is deduced from the other quantities.

The structure of the plasma is assumed cylindrical, the values of the plasma densities are given as an analytic function with a smooth transition to the natural electronic density of air assumed to be $10^{10} m^{-3}$. The approximate length of the diffuse plasma column is $25cm$ for a radius under $200\mu m$. The plasma domain covers the range $r \leq 600\mu m$.

5. The observed effects.

Table 1
Some order of magnitude.

Fluid heating by plasma (s)	10^{-7}
Density remains unchanged (s)	10^{-6}
Pressure equilibrates (s)	10^{-5}
Formation of low density channel (s)	10^{-5}
Expansion of the bow shock (s)	10^{-2}
Positive effects on the fluid (s)	10^{-1}

These numbers illustrate that the considered phenomena occur on disparate time scales.

5.1. The initial fluid state

We compute a stable state for a truncated quasi-realisatic profile put under an incoming fluid at Mach 3. The plane profile is constructed analytically, which proves to be useful during mesh generation. The fluid is considered as an ideal gas with a specific heat ratio $\gamma = 1.4$. For the presented results, the temperature of the incoming flow is taken as $260K$ while its density is $2.10^{25}m^{-3}$. The computed stable state is the fluid state prior to the instantaneous plasma appearance.

5.2. The plasma/fluid behavior during the first moments

We describe here the phenomena observed in the time window $0 < t < 3\mu s$. The density of the fluid does not change significantly during this period. The plasma recombines very fast until it reaches a state where it is not dense and hot enough to produce any significant effect on the fluid anymore. During the first microsecond the fluid remains almost steady. The evolution of the plasma depends on the fluid properties. We have a localized strong heterogeneity of the fluid characteristics due to the bow shock. On one hand, in the zone of high density and pressure behind the central part of the shock, the plasma decay is faster, while it is slower ahead of it. On the other hand, as the density of the fluid is higher behind the shock, for a same plasma state, the energy transmitted to the fluid is higher. Indeed, while the energy deposition by elastic collisions is weaker, since proportional to $T_e - T$, the global increase in energy is due to the three body recombination with a neutral. As a result of these two conflicting effects, we observe in Figure 1 the variations of fluid pressure and temperature near the shock after $3\mu s$.

In all our graphical representations, we present, except for the pressure P expressed in bar, the other state quantities will be expressed in SI units.

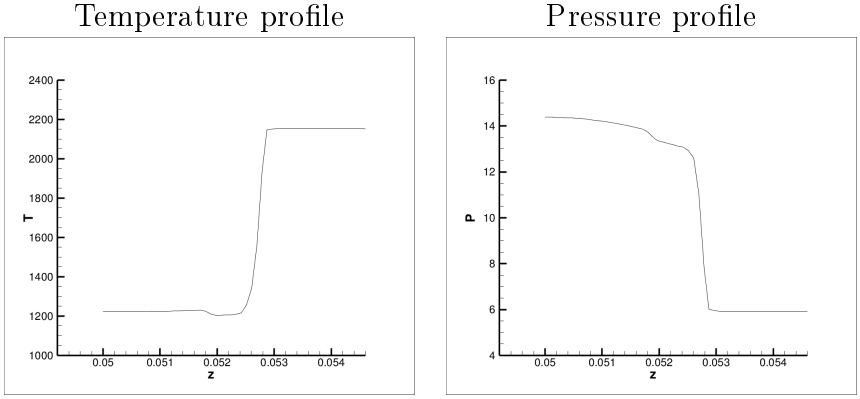

Figure 1. Profile of the shock after plasma heating at time $3\mu s$.
We see that the flow conditions inside the bow shock impedes
the fluid heating in this area.

Contrary to what happened in the initial state, in the very thin channel heated by the plasma the temperature becomes higher ahead of the shock than behind it. Let us remark that one microsecond after the introduction of the plasma, as the density remains unchanged in the heated region, the pressure shock profile is changed, as a "spike" is added to it. Let us also note that the observed effects of momentum transfer between the fluid and the plasma are not very strong. The radius of the obtained heated channel is less than half a millimeter. Due to the short life time of the introduced plasma, most of the gas temperature increase occurs during the first twenty nanoseconds.

5.3. The resulting aerodynamic effects

The resulting aerodynamic effects of the gas heating occur on a far larger time scale. After the gas heating, the overpressure in the heated central channel disappears in less than thirty microseconds. This is accompanied by the formation of a low density channel expanding radially over time.

The radius of the obtained low density channel is far from being large enough to observe any real improvement of the flight conditions due to its existence. However, the existence of this channel leads, by conservation of momentum, to a high velocity fluid income.

This thin column of fluid affects the structure of the velocity shock by locally pushing it inside. The reflected wave makes the fluid flow back. The interesting effects we obtain are a result of this phenomenon. The localization of the central part of the shock front is pushed ahead. The changes occur spatially on a scale of the same order of magnitude as the one of our truncated profile, which has a radius equal to two centimeters. The front is localized at the frontier between the two fluids flowing with opposite radial directions.

This new shock front travels ahead of the plane nose before being pushed back into initial position. Let us remark that heating locally occurs on the axis as the two fluids with opposite flowing direction meet.

As shown by Figure 2, positive effects begin to appear on the flight conditions about 15 ms after the plasma was introduced. The effects cease to be significant over 200 ms after the plasma introduction.

We obtain a drag reduction up to about 21%. These effects were produced by an energy deposited into the the fluid of about 10 mJ. As 2-D axisymmetric computations were conducted, the lower parts in Figure 3 were reconstructed by symmetry. We choose to show the fluid state at 50 ms, since the drag coefficient is reaching a minimum around this time.

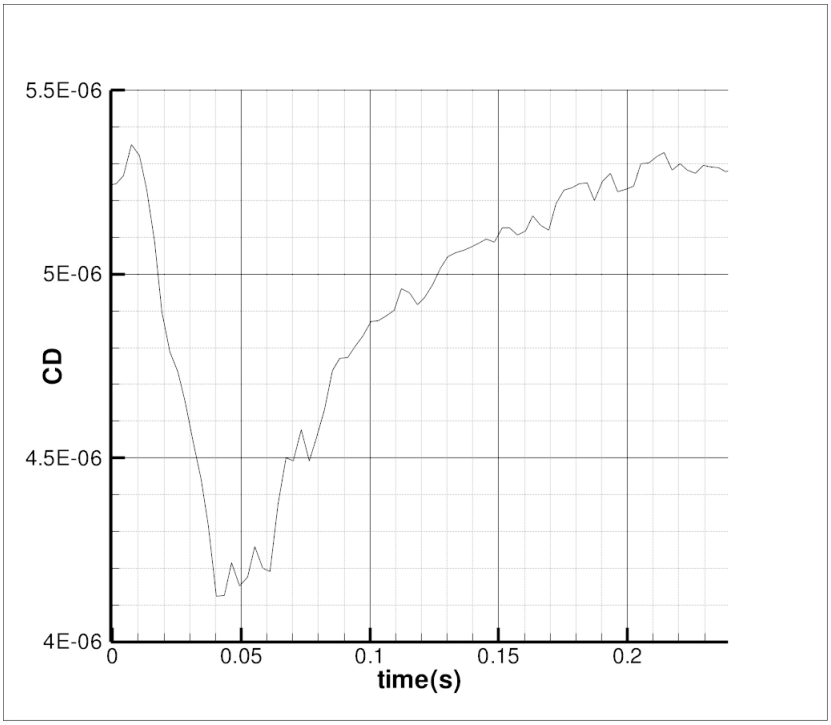

Figure 2. **Variation of the drag coefficient over time.**

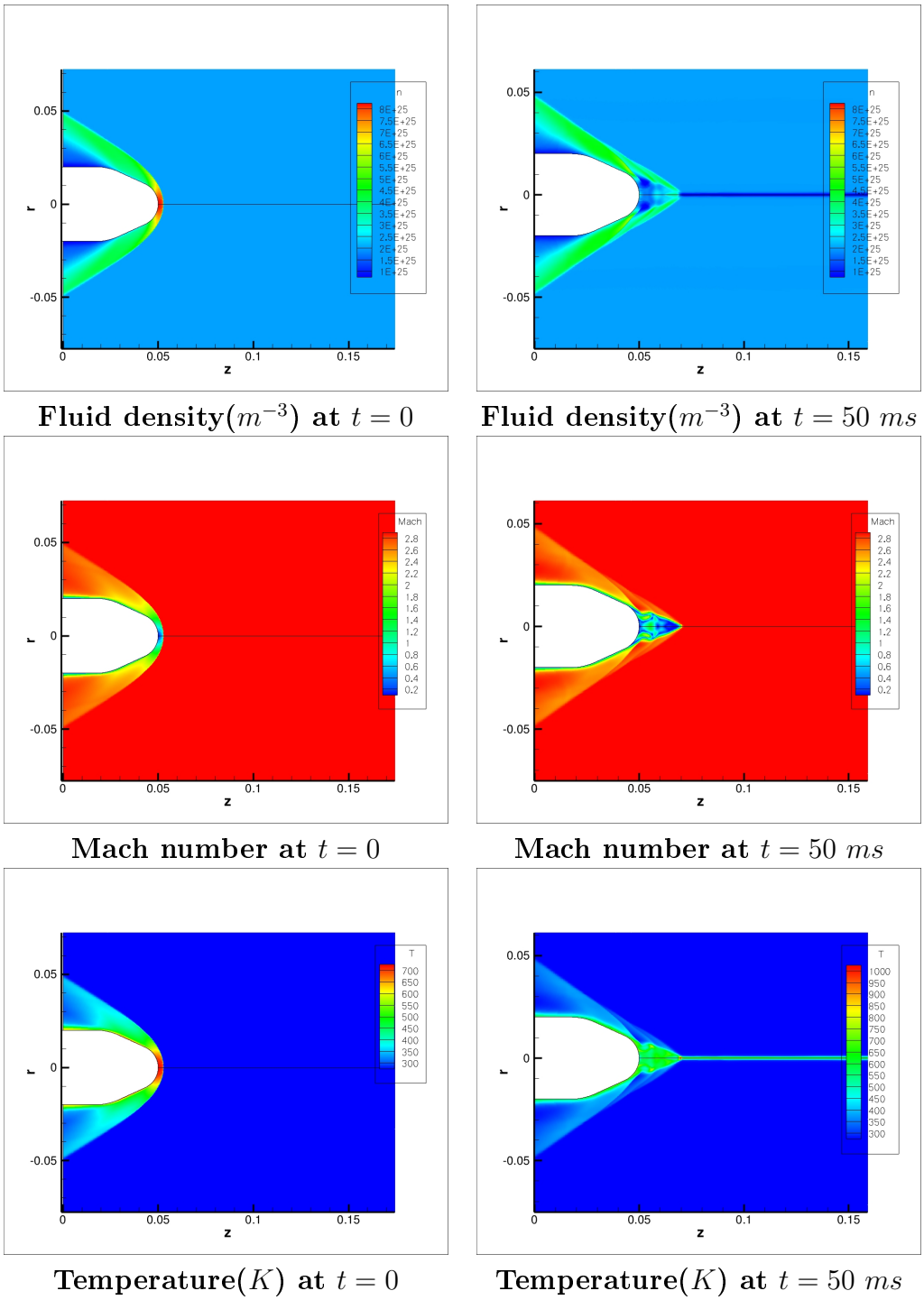

Fluid density(m^{-3}) **at** $t = 0$ **Fluid density**(m^{-3}) **at** $t = 50\ ms$

Mach number at $t = 0$ **Mach number at** $t = 50\ ms$

Temperature(K) **at** $t = 0$ **Temperature**(K) **at** $t = 50\ ms$

Figure 3. We see both the deformation of the bow shock and the decrease in the Mach number around the nose of the aircraft. We remark positive axial velocities as well as heating localized on the meeting zone of two fluid flow of opposite directions.

6. Conclusion and perspectives

Due to our simulations, we observe that although the created non-equilibrium plasma column is very thin and short-lived, it can have last longing positive effects over the fluid. In order to improve the quantitativity of our results, we have to continue to investigate the dominant physical effects governing the energetic transfer between fluid and plasma. In parallel, modelling and simulating the mechanisms hiddened for now in our initial state would be very interesting as it would allow a good estimation of energy effeciency. This extension is not so straigthforward as it would need to analyze the interaction of electromagnetism and optics with the physics presently taken into account. Finally, as the device has to be used in a pulsed fashion, we can use the proposed model, with further description of the physics if necessary, in order to test through numerical simulations how the device should be operated.

REFERENCES

1. F. Boulanger, phd Orsay university (France) (1989).
2. A. V. Gurevich, L. P. Pitaenskii, Sov. Phys. JETP 19 (1964) 870.
3. E. Hinnov, J. G. Hirschberg, Phys. Rev. 125 (1962).
4. R. Kandala, G. V. Candler, AIAA J. 42 No. 11 (2004) 2266.
5. I. Kossyi, A. Y. Kotinsky, A. A. Matveyev, V. P. Silakov, Plasma Source Sci. Tech. 1 (1992) 207.
6. K. Kremeyer, K. Sebastian, C.-W. Shu, AIAA J. 44 No. 8 (2006) 1720.
7. I. G. Girgis, M. N. Schneider, S. O. Macheret, G. L. Brown, R. B. Miles, J. Spacecraft Rockets 43 No. 3 (2006) 607.
8. M. Moisan, J. Pelletier, Book C.G.S. (2006) 429p.
9. V. M. Fomin, P. K. Tretyakov, J.-P. Taran, Aerospace Science and Technology No. 8 (2004) 411.

7. Appendix

The ionization rate ([3]) is given by:

$$\nu_i = 1.51 \times 10^{11} \sqrt{\frac{T_e}{11.6 \times 10^3}} \left(1 + 2\frac{T_e}{11.6 \times 10^3 W_i}\right) \frac{n - n_e}{N_L} exp\left(\frac{-11.6 \times 10^3 W_i}{T_e}\right),$$

For the three body recombination with a neutral particle as the third body ([5]) we take:

$$\nu_{rc,n} = 6 \times 10^{-39} \left(\frac{300}{T_e}\right)^{1.5} n_e n,$$

and for the three body recombination with an electron as the third body ([2]), we have:

$$\nu_{rc,e} = 1.71 \times 10^{-20} T_e^{-4.5} \times ln\left(1.24 \times 10^7 \sqrt{\frac{T_e^3}{n_e}}\right) n_e^2.$$